International Journal of Pharmaceutics 473 (2014) 38–54

Contents lists available at ScienceDirect

International Journal of Pharmaceutics

journal homepage: www.elsevier.com/locate/ijpharm

Implementation of an advanced hybrid MPC–PID control system using PAT tools into a direct compaction continuous pharmaceutical tablet manufacturing pilot plant

Ravendra Singh, Abhishek Sahay, Krizia M. Karry, Fernando Muzzio, Marianthi Ierapetritou, Rohit Ramachandran *

Engineering Research Center for Structured Organic Particulate Systems (ERC-SOPS), Department of Chemical and Biochemical Engineering, Rutgers, The State University of New Jersey, Piscataway, NJ 08854, USA

ARTICLE INFO

Article history:
Received 4 March 2014
Received in revised form 29 May 2014
Accepted 25 June 2014
Available online 27 June 2014

Keywords:
Model predictive control
Pharmaceutical
Continuous processing
NIR
Hybrid
PCA

ABSTRACT

It is desirable for a pharmaceutical final dosage form to be manufactured through a quality by design (QbD)-based approach rather than a quality by testing (QbT) approach. An automatic feedback control system coupled with PAT tools that is part of the QbD paradigm shift, has the potential to ensure that the pre-defined end product quality attributes are met in a time and cost efficient manner. In this work, an advanced hybrid MPC–PID control architecture coupled with real time inline/online monitoring tools and principal components analysis (PCA) based additional supervisory control layer has been proposed for a continuous direct compaction tablet manufacturing process. The advantages of both MPC and PID have been utilized in a hybrid scheme. The control hardware and software integration and implementation of the control system has been demonstrated using feeders and blending unit operation of a continuous tablet manufacturing pilot plant and an NIR based PAT tool. The advanced hybrid MPC–PID control scheme leads to enhanced control loop performance of the critical quality attributes in comparison to a regulatory (e.g. PID) control scheme indicating its potential to improve pharmaceutical product quality.

1. Introduction, background and objectives

Real time inline/online process monitoring and closed-loop feedback control systems enable the transition toward a more desirable quality by design (QbD) paradigm, rather than quality by testing (QbT) based manufacturing of the next generation of pharmaceutical products. This approach utilizes an optimal consumption of time, space and resources, while satisfying the high regulatory expectations, flexible market demands, operational complexities and economic limitations. As a closed-loop optimal control based method with explicit use of a process model, model predictive control (MPC) has proven to be a very effective control strategy over the last thirty years and has been widely used in process industries such as oil refining, bulk chemical production and aerodynamic (Singh et al., 2013a). However, in comparison to PID (proportional-integral-derivative) control, MPC is more complex to implement and is computationally expensive. Therefore, a hybrid strategy in which the advantages of both MPC and PID can be integrated is desirable. However, because of the different level of complexities associated with powder handling, the implementation of an efficient control strategy for real time product quality assurance in pharmaceutical processes is still an open area of research. The main complexities are related to the integration of different control hardwares and softwares, the integration of the plant with a centralized control platform, the real time sensing of control variables and the implementation of control-loops.

Abbreviation: QbD, quality by design; QbT, quality by testing; PAT, process analytical technology; MPC, model predictive control; PID, proportional integral derivative; PI, proportional integral; PCA, principal component analysis; NIR, near infrared; FDA, Food and Drug Administration; ERC-SOPS, Engineering Research Center for Structured Organic Particulate Systems; API, active pharmaceutical ingredient; OPC, OLE (object linking and embedding) process control; MPA, multipurpose analyzer; APAP, acetyl-*para*-aminophenol; SMCC, silicified microcrystalline cellulose; MgSt, magnesium stearate; AI, analog input; AO, analog output; PLS, partial least square; nm, nanometer; SNV, standard normal variate; PC, principal component; RMSEP, root mean square error of prediction; RSEP, relative standard error of prediction; OLUPX, online unscramblerX prediction engine; SISO, single input single output; PM, penalty on move; PE, penalty on error; ITAE, integral of time absolute error; RMSE, root mean square error; RSD, relative standard deviation.

* Corresponding author. Tel.: +1 732 4456278; fax: +1 732 4452581.
E-mail addresses: ravendra.singh@rutgers.edu (R. Singh), rohit.r@rutgers.edu (R. Ramachandran).

http://dx.doi.org/10.1016/j.ijpharm.2014.06.045
0378-5173/

Nomenclature

C_i	API composition (%)
$C_{set}(t)$	Set point (%)
$\overline{C}(t)$	Average API composition (%)
n, N	Number
K_C	Gain
K_D	Rate (s)
t	Time (s)
tf	Operation time (s)
τ_I	Reset time (s)

Currently, pharmaceutical companies are facing several challenges because of the high cost and lengthy time involved in new drug product development (approx. $1.2 billion; 10–15 years) (FDA, 2004; PhRMA, 2012; Singh et al., 2013b), reduced effective patent life, higher regulatory constraints and relatively inefficient quality by testing (QbT)-based batch product manufacturing. In recent years, the interest has grown rapidly to fully automate pharmaceutical manufacturing in order to face these challenges more efficiently (Muzzio et al., 2013). Continuous manufacturing processes operate at or near steady state, allowing for closed-loop control of the entire operation, which leads to a more robust and reliable manufacturing process. Moreover, because continuous processes reach the desired steady state in just a few minutes, they enable true quality by design (QbD)-based manufacturing. Currently, there is a high level of interest in the pharmaceutical industry in continuous-manufacturing strategies, integrated with inline/online monitoring tools, and efficient control systems. These strategies can accelerate the full implementation of the QbD paradigm for the next generation of pharmaceutical products. In addition to its flexibility and time and cost-saving features, continuous manufacturing is intrinsically steady and therefore easily amenable to model predictive design, optimization, and control methods. These methods have proven to be effective approaches to improving operational efficiency and have been widely used in various process industries. Excitingly, in the pharmaceutical industry, the application of control systems is a virgin territory, wide open to researchers and technology providers (Muzzio et al., 2013). Batch manufacturing, although traditionally used for drug manufacturing, has a number of disadvantages including the larger footprint of the equipment, higher equipment and operational costs, poorer controllability, and lower product quality (Singh et al., 2012a).

There are still different levels of complexity involved in the implementation of the control system in pharmaceutical manufacturing involving solid dosages forms. For example, integration of control hardware, software and sensors with process equipment is complex because there is no standardization of pharmaceutical equipment for control perspectives. Most of the pharmaceutical processing equipment (supplied from individual vendors) comes with standalone, black-box operating systems which are not compatible yet with the standard control platforms (e.g. DeltaV (Emerson), PCS7 (Siemens)). The consequences and challenges of controlling process variables are still not clear to the pharmaceutical companies, preventing them from investing resources in implementing control systems. Difficulties in real-time online/inline monitoring of the process variables that need to be controlled are another barrier that prevents the implementation of control systems. Near infrared (NIR) spectroscopy has raised a lot of interest in the pharmaceutical industry because it is a rapid, non-invasive analytical technique and there is no need for extensive sample preparation (Blanco et al., 1998; Lavine, 1998; Jørgensen, 2000). Spectroscopic sensors (e.g. NIR, Raman), though not new to the pharmaceutical industry, have generally not been applied for feedback control. The most suitable control strategies (PID, PI, MPC, feed forward controller, feedback controller) for tablet manufacturing processes is still unknown. Furthermore, there is no standard control package commercially available that can be employed to implement a control system in the pharmaceutical plant.

Process understanding is vital for efficient control system design and implementation. Extensive model-based (Barrasso et al., 2013a, 2013b; Barrasso and Ramachandran, 2012; Boukouvala et al., 2012, 2013; Sen et al., 2012, 2013; Sen and Ramachandran, 2012; to name a few) as well as experimental (Portillo et al., 2010; Vanarase et al., 2010, 2011; Vanarase and Muzzio, 2011) studies have been done to understand the continuous tablet manufacturing process. Few attempts have been made toward the design of a control system for the tablet manufacturing process (Singh et al., 2010a, 2012a, 2013a, 2014a, 2014b; Hsu et al., 2010a, 2010b; Ramachandran and Chaudhury, 2012; Burggraeve et al., 2012; Bardin et al., 2004; Sanders et al., 2009; Gatzke and Doyle 2001; Long et al., 2007; Pottmann et al., 2000). However, no attempts have been made to implement the advanced MPC–PID hybrid control system to a continuous tablet manufacturing pilot plant.

In this manuscript, an advanced hybrid MPC–PID control system has been implemented into continuous feeders and blender unit operations of a direct compaction tablet manufacturing pilot plant for closed-loop operation. An NIR sensor, chemometrics model and tools, a PAT data management tool, OPC communication protocols and a standard control platform have been used for real time feedback control. MPC relevant linear time invariant model has been identified in silico through step response test based on in-line real time NIR measurements. The performance of hybrid MPC–PID control scheme has been compared with basic cascade PID scheme. An additional layer of PCA based supervisory control has been also added.

2. Direct compaction process

2.1. Pilot plant

A continuous direct compaction tablet manufacturing pilot plant has been installed and situated at ERC-SOPS, Rutgers University. The snapshot of the pilot plant is shown in Fig. A1 (whole plant is not shown). The pilot plant is built in three levels at different heights to take advantage of gravitational material flow. The top level is used for feeder placement and powder storage, the middle level is used for delumping and blending, and the bottom level is used for compaction. Each level consists of a 10×10 square feet working area. There are three gravimetric feeders -with the capability of adding more- that feed the various formulation components (API, excipient etc.). A co-mill is also integrated after the feeder hopper primarily for de-lumping the powders and creating contact between components. The co-mill eliminates any large, soft lumps within the powder. The lubricant feeder is added after the mill to prevent over lubrication of the formulation in the mill. These feed streams are then connected to a continuous blender within which a homogeneous powder mixture of all the ingredients is generated. Subsequently, the outlet from the blender is fed to the tablet press via a rotary feed frame. The powder blend fills a die and is subsequently compressed to create a tablet.

2.2. Process description

A flowsheet model description of the direct compaction continuous tablet manufacturing process is shown in Fig. 1. The

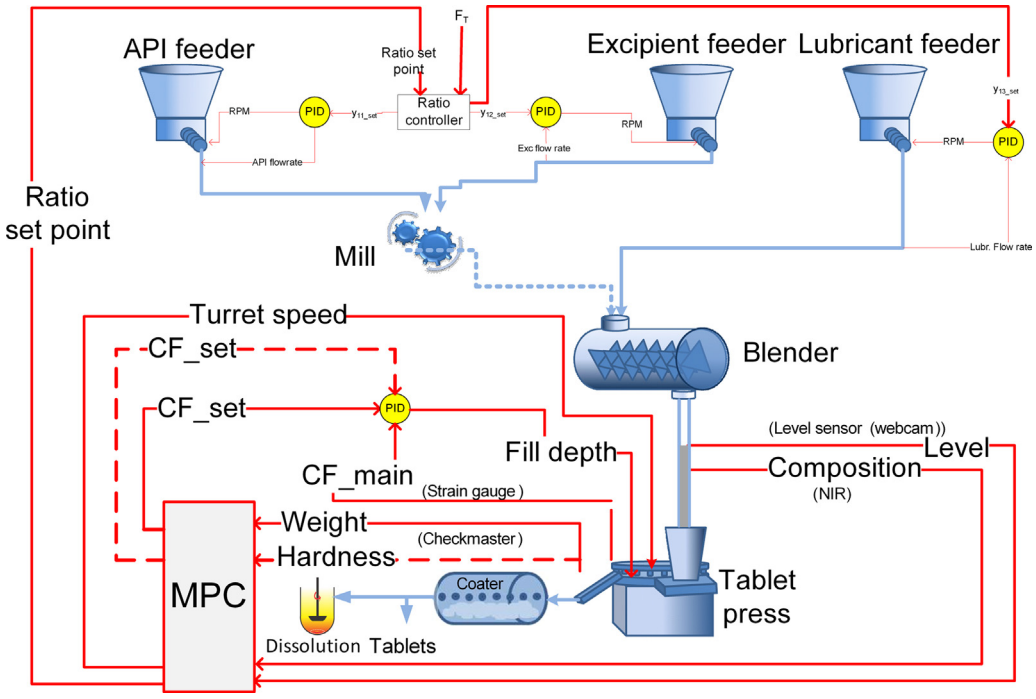

Fig. 1. Direct compaction tablet manufacturing process and control architecture.

process schematic represents a pilot plant situated at the Engineering Research Center for Structured Organic Particulate Systems (ERC-SOPS), Rutgers University. Details of the process dynamics of the pilot plant have been previously reported (Vanarase and Muzzio, 2011), and the open-loop operation has been extensively studied (Boukouvala et al., 2012; Boukouvala et al., 2013; Portillo et al., 2009, 2010; Vanarase et al., 2010; Vanarase et al., 2011).

The process flowsheet as shown in Fig. 1 has been simulated using the simulation software gPROMS (Process Systems Enterprise, http://www.psenterprise.com). The integrated flowsheet model for direct compaction continuous tablet manufacturing process that has been used for design of the control system has been previously reported (Boukouvala et al., 2012, Singh et al., 2013b). The detailed developments of these models are reported elsewhere as summarized here. The mathematical model for milling (Barrasso et al., 2013a, 2013b) and powder blending, an important but complex unit operation, has been previously developed (Sen et al., 2012, 2013; Sen and Ramachandran, 2012). The model for the tablet compression process is previously reported in Singh et al. (2010a). This model is based on the Kawakita powder compression model (Kawakita and Ludde, 1971) and tablet hardness model described in Kuentz and Leuenberger (2000). The dissolution model was adapted from Kimber et al. (2011). The models for the different unit operations have been developed and included in gPROMS library to facilitate the integrated flowsheet modeling. The development of the integrated process flowsheet using individual unit operation models has been previously demonstrated (Boukouvala et al., 2012, 2013). The models involved in direct compaction tablet manufacturing process and the references related to model development and validation are listed in Table A1.

3. Advanced hybrid MPC–PID control strategy for continuous tablet manufacturing process

In a hybrid MPC–PID control structure, the MPC is placed at supervisory level under which PID is placed as slave controller. The basis of hybrid control scheme is given in Appendix A2.

3.1. Advanced hybrid MPC–PID control architecture and real time monitoring tools

The process flowsheet model (Singh et al., 2013a) has been used to design the control system for direct compaction continuous tablet manufacturing process prior to implementation into pilot plant. The model-based control system design is a systematic procedure that includes the identification of the critical control variables, pairing of control variables with suitable actuator, identification of the suitable control algorithm, controller parameters identification and finally implementation of the control strategy into a process model for controller performance evaluation (Singh et al., 2009, 2010a, 2012a, 2013a, 2014a, 2014b). The configuration of the designed control scheme together with real time monitoring tools for the direct compaction continuous tablet manufacturing process is shown in Fig. 1. The list of key control variables, corresponding manipulating variables and sensors are listed in Table 1. An ontological knowledge-based system for selection of monitoring tools has been previously reported (Singh et al., 2010b). A combination of model predictive control (MPC) and the more commonly used proportional integral derivative (PID) is used for the control strategy since MPC is better at handling process delays and process variable interactions and can be tuned easily. An NIR sensor was placed at the blender outlet for blend composition measurement. This is the input for the master controller, which generates the feeder ratio set point. Based on this

Table 1
Key control variables, corresponding manipulating variables and sensors.

Key control variables	Manipulating variables	Sensors
API composition	Ratio set point	NIR
Powder level in instrumented hopper	Turret speed	Webcam
Tablet weight	Fill depth	Check master (Fette)
Tablet hardness	Fill depth (shared)	Check master (Fette)

ratio set point and the total powder flow rate, the individual flow rate set points for API, excipients and lubricant feeders are calculated and then controlled by manipulating the respective feeder RPMs using built-in feeder controllers based on PID logic. In continuous manufacturing, the powder needs to flow continuously through each unit operation, therefore, there is no holding step involved in the current setup of the pilot plant to make sure that the composition reaches the target before going into next step. Therefore, we need the real time feedback control system to make sure that the composition is always within the specified tolerance limits. However, if the composition violates the specified tolerance limits because of any reason (e.g. blockage) then the blends need to be diverted in real time for that interval of time and corrective actions need to be taken to bring back the blend uniformity within specification. The instrumented hopper level (placed in between blender and tablet press) is controlled by manipulating the turret speed. The hopper level is monitored by webcam. Webcam takes the image of powder level in real time and passes it to the MATLAB image analysis toolbox. MATLAB converts the picture to univariate signal. This is then compared against two calibration points. One point is the value when there is no powder in the instrumented hopper (chute) and one when the chute is full with powder. The first value is 0% level and the second is 100% level. Where the live value falls between the two calibration points is the calculated level. The level % is then sent to DeltaV via MATLAB OPC toolbox as the input to MPC block. The level set point is 50%.

In the tablet press, the tablet weight and hardness are controlled through a cascade control arrangement using two master loops and one slave loop. Master loops are used to control the weight and hardness and provide the set point for the slave controller, which controls the main compression force by manipulating the fill depth. They share a common slave controller, meaning that only one master controller is activated at a time. The tablet weight is measured and controlled more frequently. Note that the hardness control loop is activated only when the measured hardness deviates by a certain percentage (e.g. 2% of set point) from the desired set point. This is standard Fette (equipment company) tablet press approach to control tablet weight and hardness. Check master (Fette) has been used for tablet weight and hardness measurement in real time. With the current state of the art sensing techniques, the content uniformity in the final tablets cannot be measured in real time (in-line/on-line). However, it can be measured at-line. For example, an MPA (Bruker) can be used for at-line measurement of tablet content uniformity. The continuous manufacturing is known to handle the segregation issues of materials well and therefore, a good agreement between blend composition and tablet content uniformity is expected.

3.2. Coupling of PCA based supervisory control system with the hybrid MPC–PID control architecture

A PCA based supervisory control system has been coupled with the hybrid MPC–PID control system to ensure that the NIR prediction is acceptable for feedback control purposes. This integration was performed only for the control variables (e.g. API composition) where the spectroscopic sensors has been used for monitoring. UnscramblerX Process Pulse (CAMO) platform has been used to calculate the PCA based statistics (e.g. scores, Hotelling's T^2 and Q residual etc.) in real time and then these values are passed to DeltaV (Emerson) via synTQ (Optimum). Process pulse communicates with synTQ via its established coupling features while synTQ communicates with DeltaV via OPC communication protocol.

A score plot has been used to measure the total variance in the data with respect to a calibration set. The score plot provides qualitative means to trend the variance in sample data. It can also serve as a visualization of the similarity of samples with respect to each other, when viewed either as a line or a 2D scatter plot. For similar samples, if the data points are less scattered and within the ellipse space then it can be consider as a good prediction. If significant amount of data points are outside the ellipse area then it means that the sample data does not match with the calibration set and prediction may not be reliable and therefore the process needs to be stopped and either powder material need to be rechecked for any operational mistake (e.g. incorrect excipient, feeder malfunction) or the prediction model needs to be recalibrated. Hotelling's T^2 statistics is used to detect process deviation, potential process upsets or other measurement issues. The Hotelling's T^2 limit is calculated based on the calibration samples, and is based on a user-specified significance level (e.g. 1.0, 5.0, 10.0% etc.). The limit is used to detect the outlier for newly measured samples. Data points that violate this limit are considered as the outliers and need further investigation. The contribution plots for the Hotelling's T^2 plot related to these outliers need to be analyzed to identify the root cause of an outlying sample. Another valuable outlier detection statistic that has been used is the Q residuals, which are related to the variance in the variables (e.g. a sample spectrum) that is not explained by the model being used. The Q residual limit has been also calculated based on calibration samples and user specified significance level. The samples violating the Q residual limits could be outliers and need further investigation to identify the root cause of violation. Contribution plots indicate the contribution of each variable to a measured statistics (Hotelling's T^2, Q residuals) and therefore can be used to identify the variables that cause the violations. The model's average values of these statistics have been compared with the calculated statistics to identify the root causes of violation. The higher contribution value of the statistics corresponding to a particular variable is an indication of the problem with that variable. In case of any violation of Hotelling's T^2 and Q residual limits, first the warning is displayed on control user interface, then an alarm is generated and finally the actions have to be taken. The PCA based supervisory control helps to avoid sending faulty data to the control loops and to take the appropriate corrective actions.

4. Control hardware and software integration

The control hardware and software required for implementation of the control system are integrated with the plant for real time monitoring and closed-loop operation (Fig. 2). The feeders and blender have been considered here as a demonstrative example. The complete automation has been achieved through three stages. In stage 1, the plant hardware/unit operations are connected with the control platform so that they can be operated through a centralized control interface. Standard industrial communication protocols such as Fieldbus or EtherNet/IP can be used to make these connections (Blevins et al., 2013). Through this connection, the actuator signals can be sent to the plant as an input. For example, DeltaV (Emerson) control platform has been integrated with feeders (Schenck) via DeviceNet and with blender (Gericke) via serial ports to facilitate automatic operation. In stage 2, the inline/online sensors have been integrated with the plant and control platform for real time process monitoring. For example, an NIR sensor has been integrated at the blender outlet to monitor API composition through a suitable sampling interface and with the computer through operating software. The measured signal is then sent to the control platform. This step includes the development of a calibration model (for example, see Vanarase et al., 2010), the integration of the sensor operating software with the online prediction tools, the integration of the inline/online prediction tools with the PAT data management tool

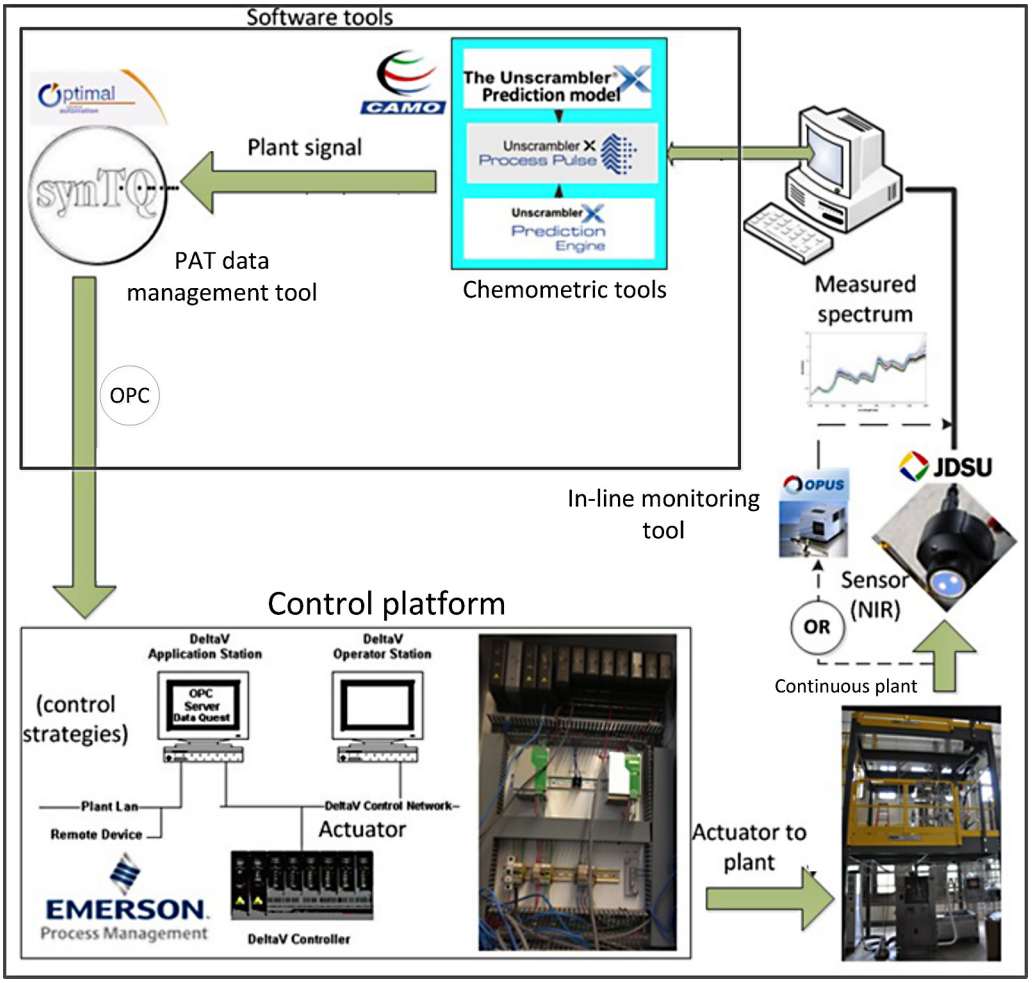

Fig. 2. Example of control hardware and software integration.

and the integration of the PAT data management tool with the control platform via the OPC communication protocol. Through this step, the measured signal and any other signals (e.g. alarms, warnings, etc.) can be sent to the control platform to be recorded in the historian, and any data from the control platform can be sent back to the PAT data management tool for data storage, inspection and auditing purposes. In stage 3, the control-loops have been added for automatic feedback plant operation. The control-loop connects the plant input (actuator) with the plant output (control variable) through a control algorithm. The input for the controller comes from the sensors and the output from the controller goes to the plant. An example of control hardware and software integration is shown in Fig. 2. As shown in figure, a micro NIR sensor (JDSU) has been used for API composition

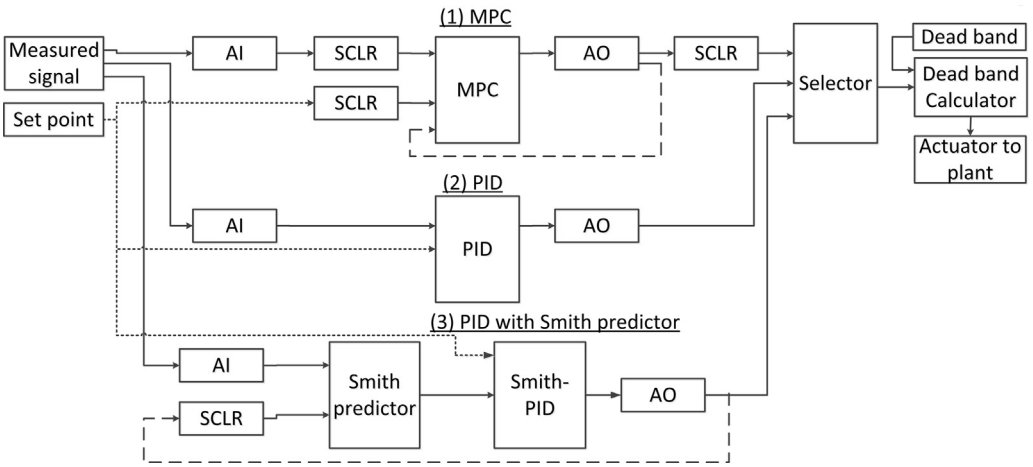

Fig. 3. Implemented controller for drug concentration control (AI: analog input, AO: analog output, SCLR: scale-up/down). (1) MPC route, (2) PID route, (3) PID with dead time compensator route.

measurement. The NIR calibration model is developed in UnscramblerX (CAMO) and Process Pulse and OLUPX prediction engine (CAMO) are used for real time prediction of API composition. A PAT data management tool (synTQ) is used for data management and storage. An OPC communication protocol is used to communicate the signal between PAT data management tool and control platform. The control strategy is implemented in the control platform and calculates the actuators which are sent to the plant.

5. Materials and methods

For this study, the excipient and lubricant are placed in a single feeder and API in a different feeder. In the first feeder APAP (acetyl-*para*-aminophenol) (API) is filled and in the second feeder silicified microcrystalline cellulose (SMCC) (excipient) mixed with 1% magnesium stearate (MgSt) (lubricant) is filled. SMCC and magnesium stearate are pre-blended using a batch blender (Glatt) before being fed to the feeder. The concentration of excipient is significantly greater than that of the lubricant. Loss-in-weight feeders (Schenck) have been used. The feeders consist of a hopper, a load cell that is integrated with a gravimetric controller and a conveying screw. A co-mill (Glatt) is used for delumping purposes. Conical screen mills consist of a cone shaped screen with an impeller inserted into the center. The impeller rotates and material is ground between the impeller and the screen until it is small enough to pass through the holes in the screen and leave the mill. The total inlet flow rate of co-mill is fixed to 20 lb/h. A continuous convective blender (Gericke), in which the primary mixing mechanism is convection induced by rotating blades (Portillo et al., 2008) has been used. The blender speed is fixed to 30% of the maximum speed. The total inlet flow rate of the blender is 20 lb/h. A cylindrical chute is used to interface with the NIR for real time data collection. MicroNIR™ 1700 Spectrometer (JDSU) has been used to measure the API composition at blender outlet. This is an ultra-compact, lightweight NIR tool that relies on a linear variable filter (LVF) as the dispersing element and uses advanced coating design and manufacturing technology. The wavelength range of this NIR sensor is 950–1650 nm, typical measurement time is 0.5 s, minimum integration time is 10 μs and the optimum sample distance from detector is 3 mm. For this study, the optimal acquisition parameters were defined as: integration time 40,000 μs, the number of samples averaged per scan 50 and 1 s for time between scans. IRSE (JDSU) software is used to operate the MicroNIR. 100% reference was set by placing MicroNIR in contact with spectralon (99% reflectance) and zero reference was set by pointing it away from the light. Normalized reflectance values are computed from the dark, raw 100% reference and raw sample scans as follows: normalized = (sample − dark)/(reference − dark). Data are automatically exported to "Process Pulse (CAMO)" chemometric software for real time prediction. A partial least square (PLS) based model developed in UnscramblerX and a prediction engine (OLUPX) are used for real time NIR prediction needed to take the control action. Control limits of ±0.15 of set point have been provided as the acceptable limits.

6. Implementation of a model predictive controller (MPC)

The control variable, "API composition" has been considered for the demonstration of control loop implementation. The control strategy has been implemented in DeltaV using its control studio feature. The MPC toolbox of DeltaV has been used to implement a supervisory MPC controller above an inbuilt PID based feeder controller. The implemented MPC controller is shown in Fig. 3. A simpler PID controller and PID with a Smith predictor have been also implemented as shown in Fig. 3. Therefore, the implemented controller is a flexible system connected with a switch button so that the user can select one

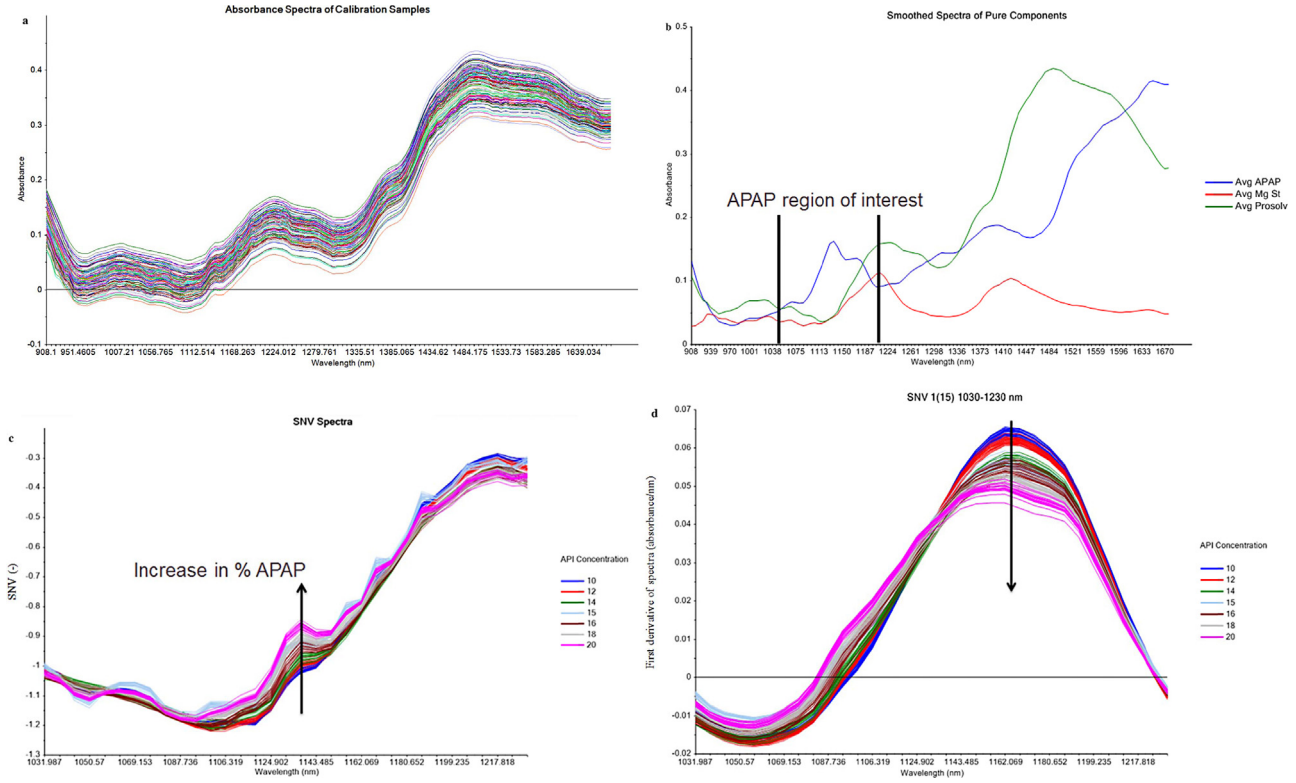

Fig. 4. Development of NIR calibration model. (a) Absorbance spectra of calibration samples. (b) Smoothed spectra of pure components. (c) SNV spectra. (d) First derivative of spectra.

control scheme at a time. PID is the simpler control scheme. The Smith predictor introduces the dead-time compensator into the PID algorithm. MPC is an advanced controller that has several advantages over the PID controller. In Fig. 3, the MPC loop is shown at the top, the PID loop is shown in the middle and the PID with the Smith predictor is shown at bottom. As shown in the figure, the ratio set point (CAS_SP) and the measured composition (API-C) are the inputs to the MPC, PID and Smith predictor blocks that generate the actuator which goes to a selector block. The measured signal (from NIR) is obtained from Process Pulse and synTQ through OPC communication protocol. The measured signal goes to analog input block (AI) and output of AI block is input of controller block. The controller output (actuator) goes to the analog output (AO) block and the output of AO block goes to a selector block. Note that in MPC scheme (see top of Fig. 3), the scale-up blocks before and after MPC block have been added to scale-up the fractional composition signal to the percentage composition signal before entering to the MPC block and scale-down the MPC output signal again before sending to the plant because at higher scale MPC performs better. The scale-up blocks are not needed in PID and Smith predictor schemes. The selector block has three total inputs. The first input comes from the MPC block, the second input comes from the PID block, the third input comes from the PID with the Smith predictor block. One of these options will be selected by the selector block. For example, if the user has selected the MPC, then the first input will be selected. After the selector block, this input will enter a calculator block where the dead band has been integrated. The dead band is used to ensure that the controller output lies within a range. After this block, the output goes to the ratio controller. The ratio controller calculates the flow rate set points for the API and excipient feeders based on the ratio signal and the total flow rate. The API and excipient flow rates are then controlled through the internal PID controller by manipulating the screw rotational speed. The screw rotational speed is sent to the plant from DeltaV using DeviceNet.

7. Real time inline monitoring of API composition for feedback control

The API composition has been monitored inline using a MicroNIR sensor placed at the blender outlet through the window of a cylindrical chute. From the collected spectrum, the API composition is predicted using OLUPX 10.2 (CAMO) online prediction tool and a PLS calibration model. To develop the calibration model, the pre-blended samples of 10%, 12%, 14%, 15%, 16%, 18% and 20% APAP were prepared. The sample consists of APAP, SMCC and 1% magnesium stearate. Raw spectrum data and pre-processing of the data is shown in Fig. 4. As shown in Fig. 4a, the absorbance spectrum for these calibration samples in the 900–1700 nm wavelength range has been collected. The collected spectrum is then exported to the model development software (Unscrambler X (CAMO)) to perform pre-processing, PCA and to build the PLS model. The smoothed spectrum of pure component (APAP, SMCC, MgSt) is plotted in Fig. 4b. Based on a pure component spectrums analysis, the wavelength region of interest for APAP has been identified to be 1030–1230 nm which has been used to develop the PLS model. To reduce the influence of particle size, scattering and other influencing factors (Candolfi et al., 1999), the raw data is pre-processed. Varying particle sizes result in a baseline shift in the spectra, because the particle size defines the spectral pathlength. Fig. 4c shows the standard normal variate (SNV) transformation. SNV transformation has been used to removes the baseline differences from spectra caused by scatter and variation of particle size (Barnes et al., 1989; Candolfi et al., 1999). The transformation is applied to each spectrum individually by subtracting the mean spectrum and dividing by the standard deviation. By calculating the derivative spectra, overlapping peaks have been deconvoluted and the chemical differences enhanced (Osborne et al., 1993). Fig. 4d shows the first derivative of spectrum. The figure shows that the peak of each composition is separated and is in increasing order.

PCA – a tool to reduce multidimensional data to lower dimensions while retaining most of the information- has been used to analyze the raw data (Osborne et al., 1993). PCA uses projections to extract from a large number of variables, a much smaller number of new variables, which account for most of the variability between samples (Jørgensen, 2000). Each of the new variables (principal components) is a linear combination of the original measurements and therefore contains information from the entire spectrum. PCA fits new axes (variables) in the data space. The first axis is chosen in the direction of maximum variability. This way the amount of information in the first new variable is maximized. The second axis is chosen to be orthogonal to the first, so the second new variable is uncorrelated with the first one. This operation is continued until a sufficient amount of variation is explained by the new variables. The PCA scores plot of the calibration samples pre-treated with an SNV and Savitzky Golay first derivative with 15 smoothing points in the spectral region of 1030–1230 nm is shown in Fig. 5. As can be seen from the in figure, PC1 explains 91% variance while PC2 explain 8% variance. Each data point in the scores plot represents a spectra and one color

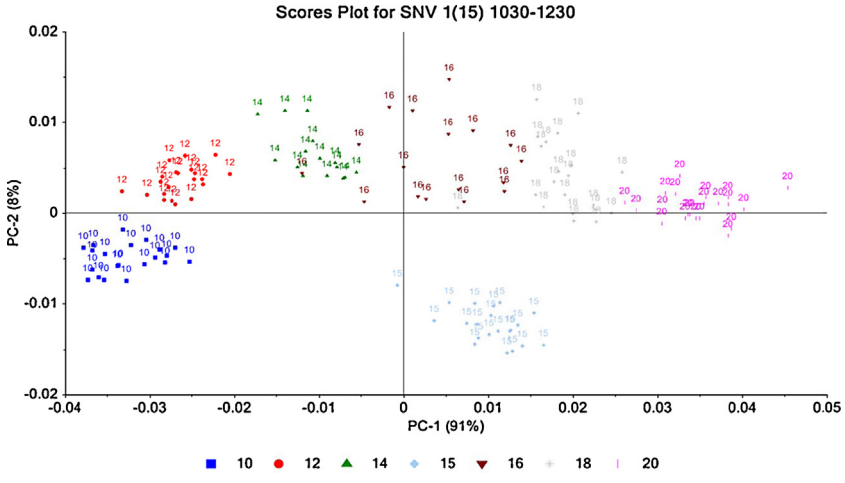

Fig. 5. PCA scores plot.

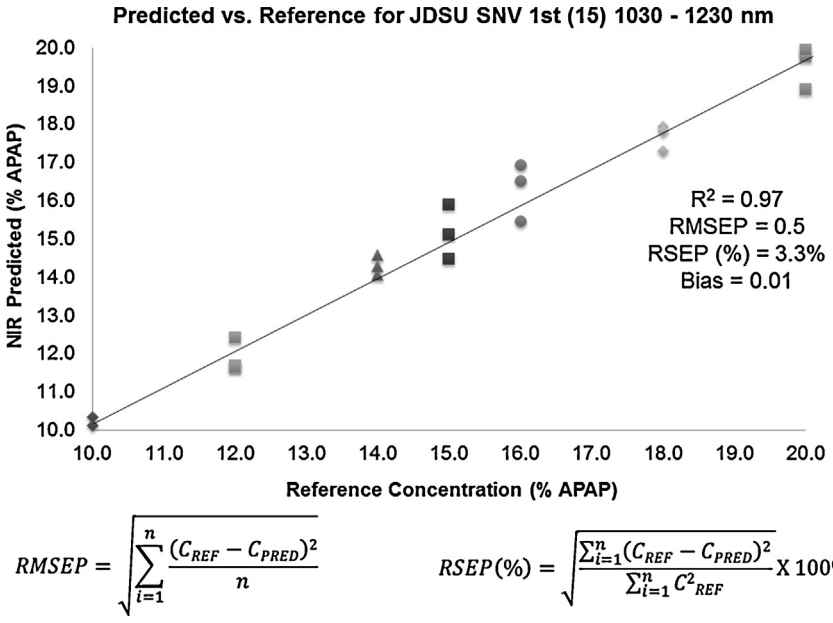

$$RMSEP = \sqrt{\sum_{i=1}^{n} \frac{(C_{REF} - C_{PRED})^2}{n}} \qquad RSEP(\%) = \sqrt{\frac{\sum_{i=1}^{n}(C_{REF} - C_{PRED})^2}{\sum_{i=1}^{n} C^2_{REF}}} \text{ X } 100\%$$

Fig. 6. PLS NIR calibration model validation. RMSEP = 0.5; RSEP = 3.3%.

represents the spectrum of a particular API composition. As desired for a good calibration model, the spectrum of each API composition is clearly separated in the score plot except very minor overlapping between spectra of 14% and 16% API composition (see Fig. 5). For each API composition the within variation among spectra is very low. Changing from PC2 to PC3 increases explained variance by only 1.3857% therefore two principal components have been selected. Further evaluation (loadings) also confirms that at 3PCs over fitting occurs (result is not shown here).

The developed PLS calibration model has been validated using a separate validation set of samples. Fig. 6 shows the actual API composition and the predicted API composition. As shown in the figure, the model predicts the API composition with reasonable accuracy. The root mean square error of prediction (RMSEP) is 0.5, relative standard error of prediction (RSEP) is 3.3% and bias is 0.01. The developed NIR calibration model is then imported to Process Pulse (CAMO) for real time API composition prediction using OLUPX (CAMO) prediction tool.

8. Linear MPC model identification, controller generation and MPC parameter tuning

The linear model required for MPC is generated using the DeltaV predict feature. As shown in Fig. 7, the step changes in input variables are introduced and based on the effect on output variables, the linear model is generated. A ±3% step change in input variable (actuator) from nominal value and a guessed time to steady state (480 s) have been provided as the inputs. Nominal value of actuator is provided as 15 (% API composition). The duration of the linear model generation test is based on the estimated time to steady state and determines the maximum time duration of pulses generated during testing. When testing is initiated, the controller output is automatically changed to generate a series of pulses, the duration of which changes in a pseudo-random fashion to generate the data for linear model identification (see Fig. 7). The random step and pulse changes in actuator are sent to the plant (unit operation: feeders) via

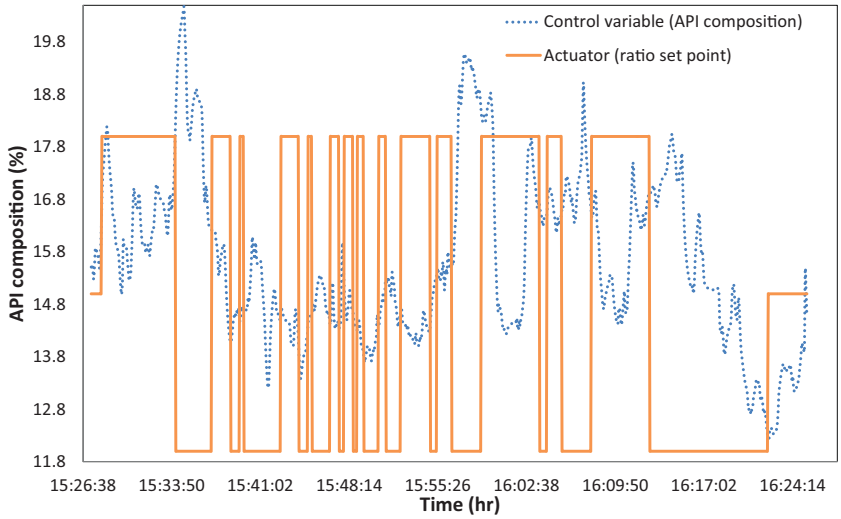

Fig. 7. Step and pulse responses of the control variable.

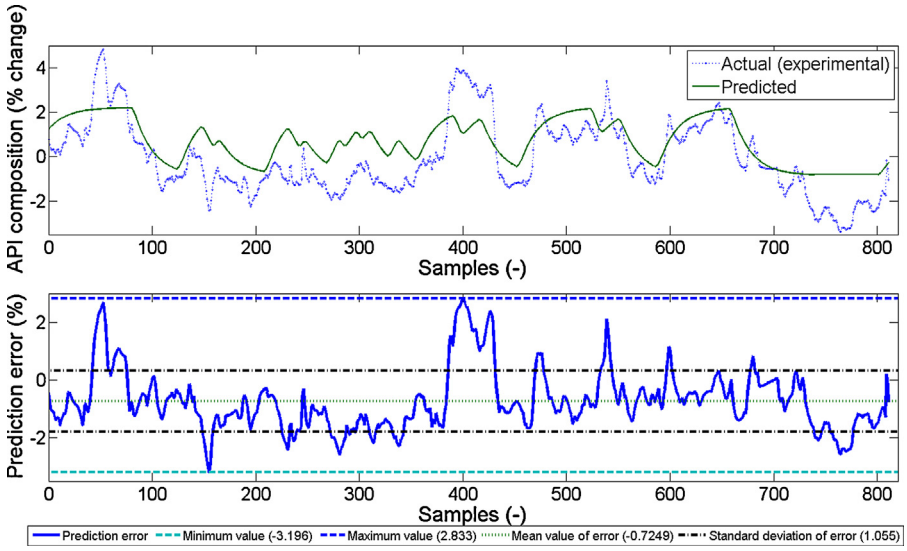

Fig. 8. Verification of linear MPC model performance. (a) Predicted vs experimental. (b) Prediction error with statistics.

DeviceNet and the corresponding API composition measured by NIR is plotted as shown in Fig. 7. A moving average of five data points (15 s of measurement) of NIR signal has been considered to smooth the signal. Based on input/output response a linear model is obtained. In this study, a SISO (single input single output) system has been considered for demonstration purposes. Fig. 7 shows that the NIR signal at blender outlet follows the ratio set point with process delays and measurement fluctuation. This figure also shows that the API composition at blender outlet could be different than the ratio set point which is input to feeders therefore external NIR based controller is needed. This deviation could be because of suboptimal performance of the load cell based inbuilt feeder controllers, any unavoidable minor inaccuracy in feeder calibration, segregation in chute, suboptimal blending, total process dead time, difference in dead times of feeders, suboptimal performance of feeders screw, minor powder blockage and any unknown disturbances. These problems can occur during manufacturing that could affect the desired API composition of the final tablet therefore this MPC based supervisory controller is proposed to reject these unknown and random disturbances.

The process dead time of the generated linear MPC model is 152 s, process gain is 0.500374, first order time constant (time required for 63.2% of final response) is 70.7099 s and second order time constant is 6.2132 s. The dead time is more than two times of first order time constant indicating that the process is dead time dominant. Note that MPC is more effective in controlling dead time dominant processes in comparison to regulatory controllers (e.g. PID). The linear model is then validated with the experimental data. The performance of the linear model is shown in Fig. 8. As shown in Fig. 8a, the linear model is able to capture the peaks of actual experimental data obtained by NIR. The square of error is 1.04924 and R^2 value is 0.7. The other statistics of the linear model performance is shown in Fig. 8b. As shown in Fig. 8b, except for few data points the error is within ±2%. As discussed in Appendix A (see Fig. A2, top) the MPC algorithm can take into account the model prediction and plant mismatch in some extent, therefore MPC is considered to be a practical approach where perfect matching of the model prediction and plant behavior is practically impossible. Increased model accuracy is however desired to improve the performance of the control system. The prediction of the linear model can be improved by increasing the magnitude of step changes and increasing the number of cycles in linear model identification process. However, increasing the number of cycles required more raw materials to run the plant for longer time and that is limited by current feeder capacity. For this plant setup, the step size (±3) was limited by the range (10–20%) of the NIR calibration model and therefore the controller output (ratio set point) has been changed only between 12% and 18%. A higher range for the NIR calibration model is desired but increasing the range an NIR model could reduce the prediction accuracy therefore this range has not been increased for this study. Using multiple NIR calibration model could be a better approach but that involves extra complexities and could be the subject of future investigation.

The MPC controller is generated using the verified process model. During controller generation in DeltaV, the MPC parameters are automatically set at an optimum value based on the process model. The linear model generated in this study has been used to tune the MPC parameters. The controller robustness can be adjusted by changing the value of penalty on move (PM). The penalty on move defines how much the MPC controller is penalized for a change in the manipulated output. High PM values result in slow controller with a wide stability margin while low PM values result in a fast controller with a narrow stability margin. With low PM settings, the control is relatively insensitive to changes in the process parameters over time or to model error. The PM value most affects the controller performance when the model does not match the real process (Blevins et al., 2013). PM is analogy to the "rate weight" terms commonly known in the control language. Penalty on error (PE) factor allows more importance to be placed on a specific controlled variable and normally known as

Table 2
Controller parameters.

Control strategy	Gain (K_C)	Reset time (τ_I)	Rate (K_D)	Penalty on move (PM)	Penalty on error (PE)	Control horizon	Prediction horizon
Hybrid MPC–PID	–	–	–	3	1	5	Inbuilt in DeltaV
PID	0.36	104.2	0.0	–	–	–	–
PID with Smith predictor	28.63	15.2	0.0	–	–	–	–

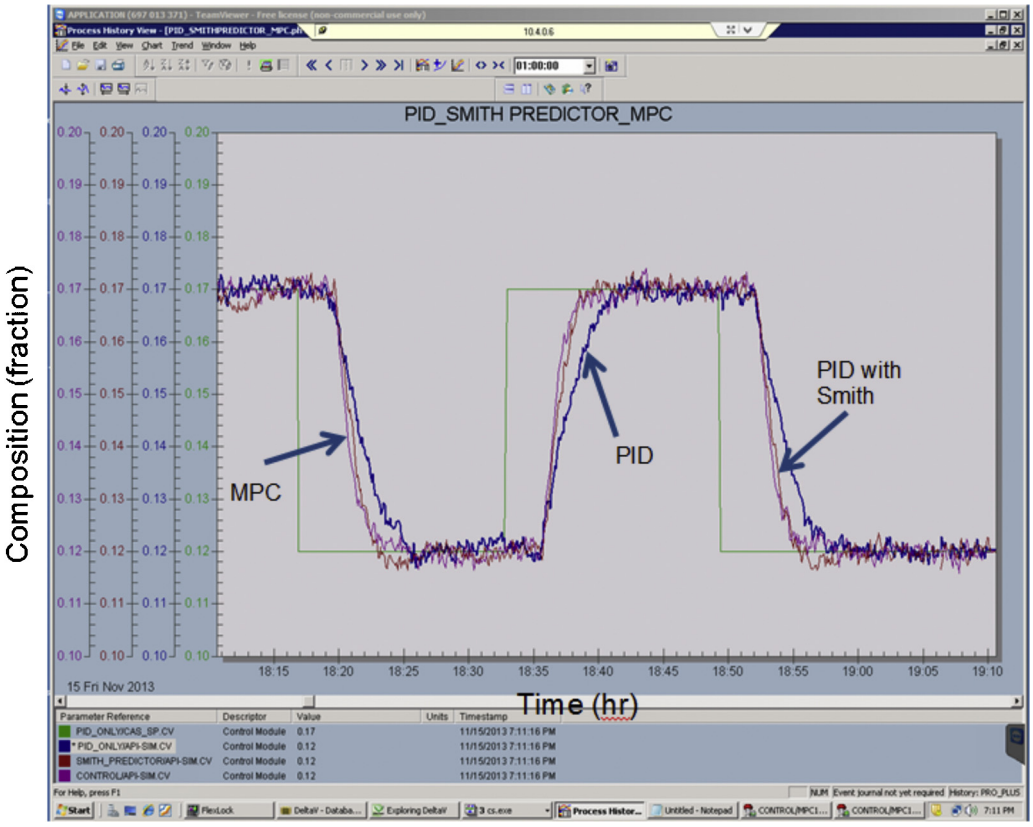

Fig. 9. Comparison of MPC performance with PID and PID with Smith predictor.

"output weight". Output weight (PE) unity and control horizon 5 has been specified for this study. In order to tune the PM, the value of PM has been changed and the MPC performance has been analyzed via the developed linear model. At PM = 3, the performance of the MPC was neither very robust nor very sluggish while at PM = 1, the MPC become extra robust which could lead to poor performance in real operational scenario. At PM = 10 the MPC is extra sluggish, that could also lead to the poor performance of the controller in actual operational scenario. Therefore, the PM value has been selected to 3. The controller tuning parameters are listed in Table 2.

For closed-loop performance evaluation, three criteria have been used. These criteria are integral of time absolute error (ITAE), root mean square error (RMSE) and relative standard deviation (RSD). ITAE, RMSE and RSD have been calculated as follows:

$$\text{ITAE} = \int_0^{\text{tf}} t|C_i(t) - C_{\text{set}}(t)|\text{d}t$$

$$\text{RSME} = \sqrt{\sum_{i=0}^{n} \frac{(C_i(t) - C_{\text{set}}(t))^2}{n}} \times 100$$

$$\text{RSD} = \sqrt{\sum_{i=1}^{N} \frac{(C_i(t) - \overline{C}(t))^2}{\frac{N-1}{\overline{C}(t)}}} \times 100$$

where $C_i(t)$ is the control variable, $C_{\text{set}}(t)$ is the setpoint, t is time, tf is the operation time, n is the total number of data point, $\overline{C}(t)$ is the average concentration, N is the number of moving data points for RSD calculation.

9. Results and discussions

The performance of the control system has been evaluated in simulation mode prior to running the actual plant in closed-loop mode. The performance of hybrid MPC–PID, PID and PID with Smith predictor control schemes are shown in Fig. 9 (simulation based). The Smith predictor is a dead time compensator (Seborg et al., 2004). The API composition set point has been changed from 17% to 12%, 12% to 17% and again 17% to 12%. To evaluate the disturbances rejection ability of the controller, unmeasured load disturbances have been also added. The random disturbances with amplitude 10 and filter time 15 have been added. As shown in the figure, the hybrid MPC–PID control system brings the API composition faster at set point, and at steady state gives the least error. As desired for a good controller, rice time is least in cause of hybrid MPC–PID controller followed by PID with Smith predictor and PID control scheme. The statistics of the control loop performance under different control schemes are given in Table 3. Integral of time absolute error (ITAE) for hybrid MPC–PID, PID with Smith predictor, and PID controllers are 4254 s, 4796 s and 5221 s respectively and RMSE values are 1.0343%, 1.3254% and 1.5263% respectively and RSD values are 0.2844%, 0.3378% and 0.4231% respectively. Therefore, hybrid MPC–PID control schemes relatively gives better performance compared to PID with Smith predictor and PID control schemes and therefore has been considered for further analysis.

Table 3
Statistical performance of different control strategies (simulation based).

Criteria	Hybrid MPC–PID	PID with Smith predictor	PID
ITAE	4254 s	4796 s	5221 s
RMSE	1.0343%	1.3254	1.5263%
RSD	0.2844%	0.3378%	0.4231%

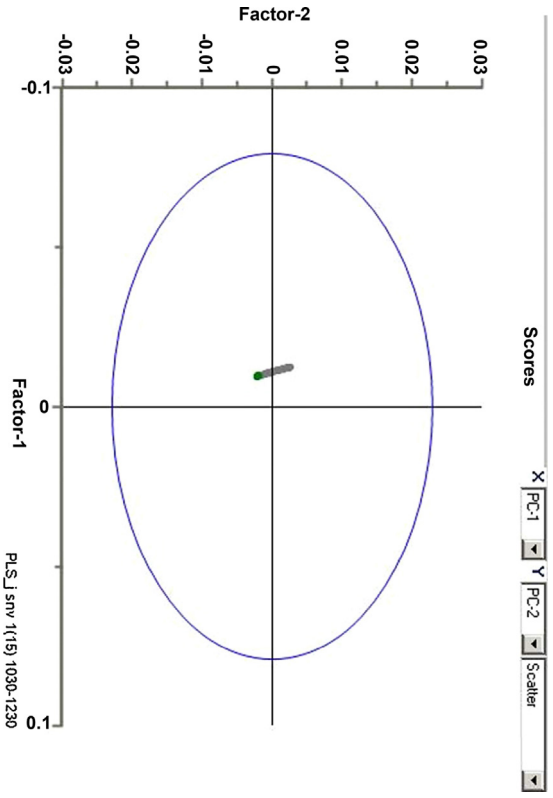

Fig. 10. Score plot obtained during hybrid MPC–PID based feedback control of the process.

Finally, the plant has been run in closed-loop scenario to validate the different integration scheme and the proposed control framework. In one feeder API (APAP (acetyl-*para*-aminophenol)) is filled and in the second feeder excipient (silicified microcrystalline cellulose (SMCC)) mixed with 1% magnesium stearate is filled. A JDSU micro NIR sensor has been used to measure the API composition at blender outlet. A PLS model developed in UnscramblerX has been used for NIR prediction. Unscrambler process pulse and a prediction engine (OLUPX) were used for real time NIR prediction. The API composition was then sent to DeltaV using OPC communication protocol. MPC uses a linear model and optimization algorithm to calculate the actuator which is then sent to a ratio controller as the input. The ratio controller then calculates the flow rate set point of API and excipient feeders. API and excipients are then controlled by manipulating the rotational speed of respective feeders. The blender speed is kept at 30% of the maximum speed.

The scores plot (for two principal components) obtained during hybrid MPC–PID based feedback control operation is shown in Fig. 10. As shown in the figure, all the data points are centralized and within the limits. The green data points are the latest data points. The figure shows that there is less variance in the data with respect to the calibration data set and there is no violation of limits. Hotelling's scatter obtained during hybrid MPC–PID based feedback operation is shown in Fig. 11a. The Hotelling's T^2 limit is calculated based on the calibration samples, and 0.5% specified significance level. As shown in the figure, no data points violate the Hotelling's T^2 limits which is an indication to the absence of outliers. Fig. 11b shows the Q residual plot. The Q residual limit has also been calculated based on 0.5% significance level and calibration sample. The figure shows that the Q residuals of the new samples are within the specified limit meaning that there are no outliers detected. Figs. 10 and 11 shows that there was no faulty data detected during hybrid MPC–PID based feedback control operation.

The different variables for example, the set point provided by the user, signals obtained from the sensors, and signals sent to the plant are then plotted in the historian of DeltaV. The closed-loop response of API composition control loop is shown in Fig. 12. The figure shows the API composition set point, API composition measured by NIR, filtered API composition signal (average of data point collected in 15 s) and the actuator response. Filtered API composition signal is the input for the model predictive controller. As shown in the figure, the API composition is controlled at 0.17 set

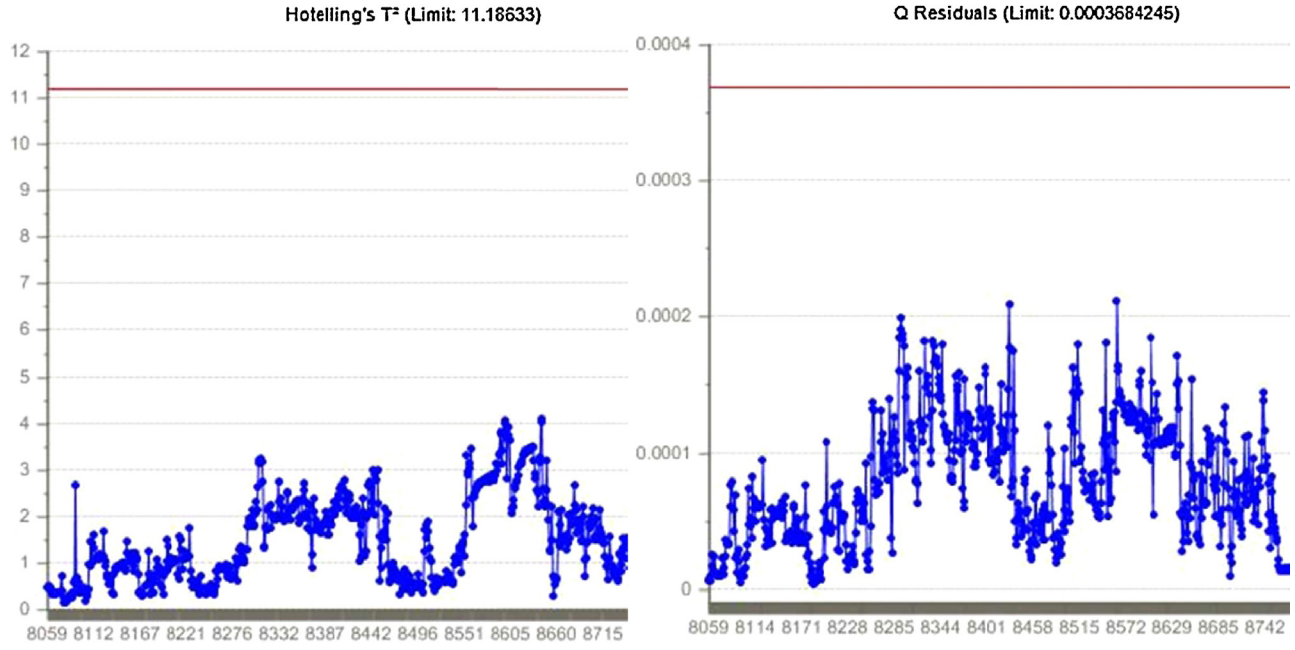

Fig. 11. Hotelling's T^2 and Q residual plots obtained during hybrid MPC–PID based feedback control of the process.

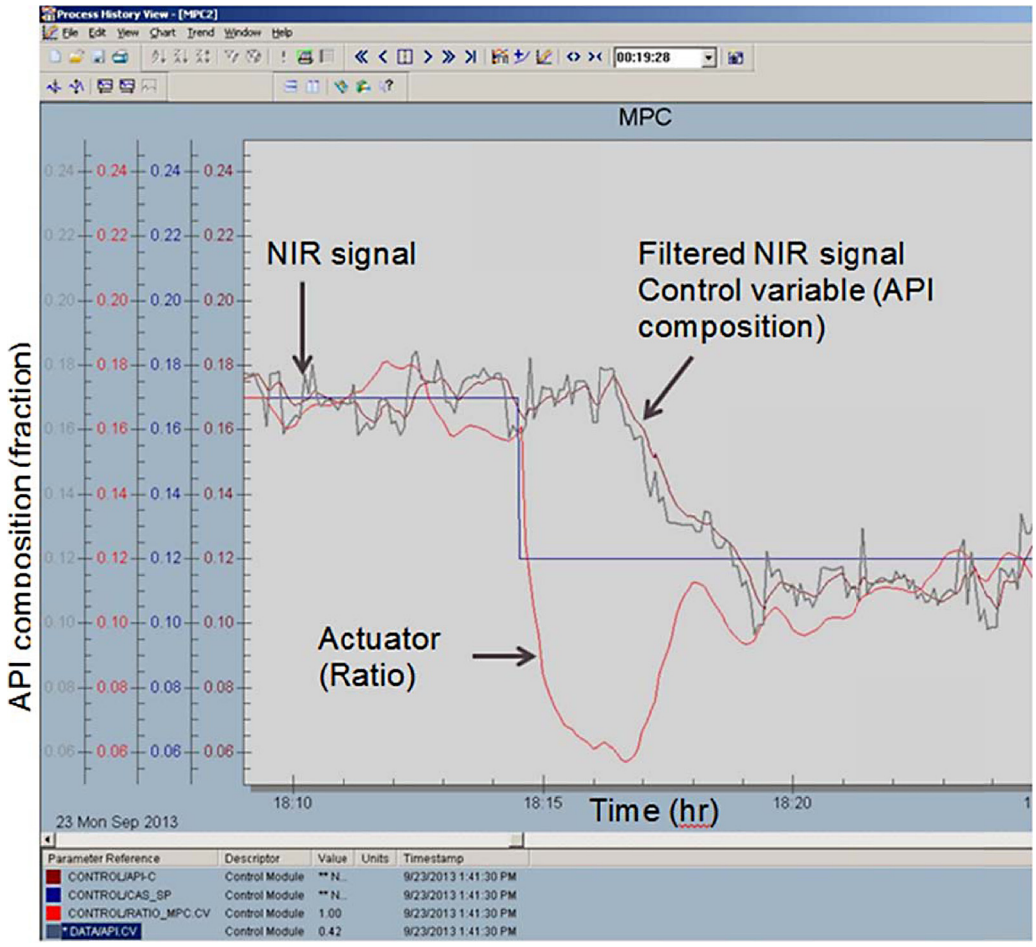

Fig. 12. Closed-loop response of hybrid MPC–PID control scheme.

point then a step change is introduced from 0.17 to 0.12. The figure shows that the controller is able to track the step change in set point. The actuator response is also reasonable. The results presented here validate that the NIR sensor has been integrated with the plant. The sensor output has been successfully communicated with the control platform (DeltaV) via OPC communication protocol. Real time online prediction of drug concentration has been made. The controller output has been communicated with the plant. The process has been verified using a fixed feeding rate. However, the process can be run at different feed rate or the feed rate can be changed during operation if needed. The feeders, mill and blender capacity are the primary limiting factors for feeding rate. Another limiting factor is the blender residence time and holdup. There should be sufficient blender residence time to ensure the desired mixing quantified by relative standard deviation (RSD). RSD limit is fixed to be 5%. The blender holdup should be consistent. To ensure the desired blender holdup, the gate valve at blender outlet can be adjusted.

The performance of slave controller is shown in Fig. 13. The excipient feeder flow rate set point and achieved profile is shown in the figure (see the top of Fig. 13). As shown in the figure, the excipient feeder flow rate oscillates around the set point with a good accuracy. In order to achieve the desired feeder flow rate, the screw rotational speed has been changed. The screw rotational speed excipient feeder is also shown in the figure. The set point and achieved profile of API flow rate is also shown in Fig. 13 (see the bottom of the figure). As can be seen in the figure, the slave controller tracks the API flow rate with good accuracy. The rotational speed of API feeder is also shown in the figure. The API and excipient feeders are of different capacity and also have the different screws to satisfy the different flow rate requirements. The excipient feeder has more capacity to hold the powder compared to the API feeder. The type of the screw has been selected based on the range of powder flow rates that need to be delivered. Excipient feeder need to deliver higher flow rate than the API feeder. Fig. 13 shows that in order to make the step change in API composition, the flow rate set point of API and excipient feeders has been changed smoothly.

The performance of the hybrid MPC–PID control system has been compared with the performance of base level PID controller in Fig. 14. In this study, the auto-tuning capability of DeltaV has been used to tune the PID controller parameters (Blevins et al., 2013). The set point has been changed from 0.17 (17% APAP) to 0.12 (12% APAP). The acceptable control limits has been specified to be of set point ± 0.15. The figure shows that the MPC response is within the control limits at 17% API composition while the PID response violates the control limits. When the step change has been introduced from 17% to 12% API the MPC brings the signal faster to the new set point in compare to PID controller meaning that MPC has less rise time in compare to PID. At the new set point, the MPC response is within the control limits except very minor violation at two points. PID controller has been selected for comparison to analyze the advantages of advanced hybrid MPC–PID control scheme compared to basic level controller. Note that the performance of both hybrid MPC–PID and PID control schemes can be further improved by integrating the other performance improvement techniques and tools. For example, integrating Smith predictor (dead time compensator) could

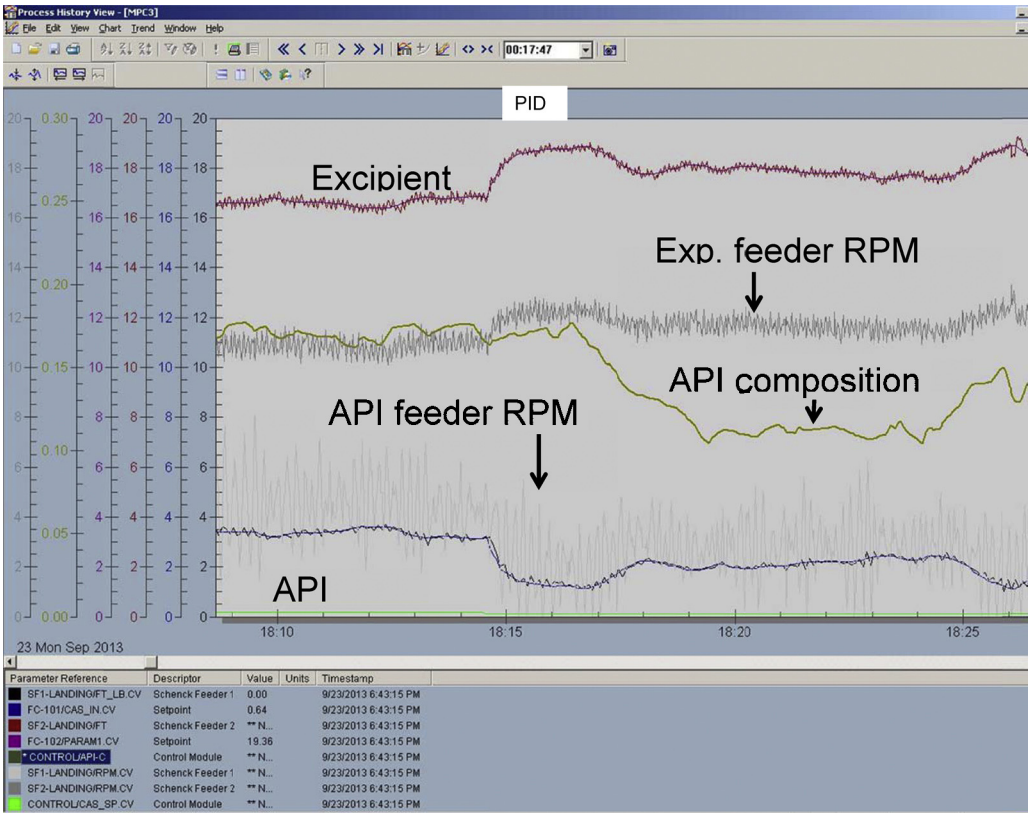

Fig. 13. Performance of slave controller.

improve the performance of PID controller. However, the performance of Smith predictor is very dependent on the accuracy of the process model. Any model-process mismatch can lead to poor performance of the Smith predictor based PID controller and therefore in powder handling complex process where a perfect process model is difficult to develop, the practicality of Smith predictor is limited and subject of further investigation.

The deviation of achieved profile from the set point is shown in Fig. 14. As shown in the figure, the MPC error is within the acceptable limit except for a short duration where a step change has been made. The powder at blender outlet needs to be diverted for this short period of duration. In the case of PID, the error violates the acceptable limits during most of the operating period. To quantify the performance of hybrid MPC–PID control scheme, the integral of time absolute error (ITAE (Seborg et al., 2004)), root

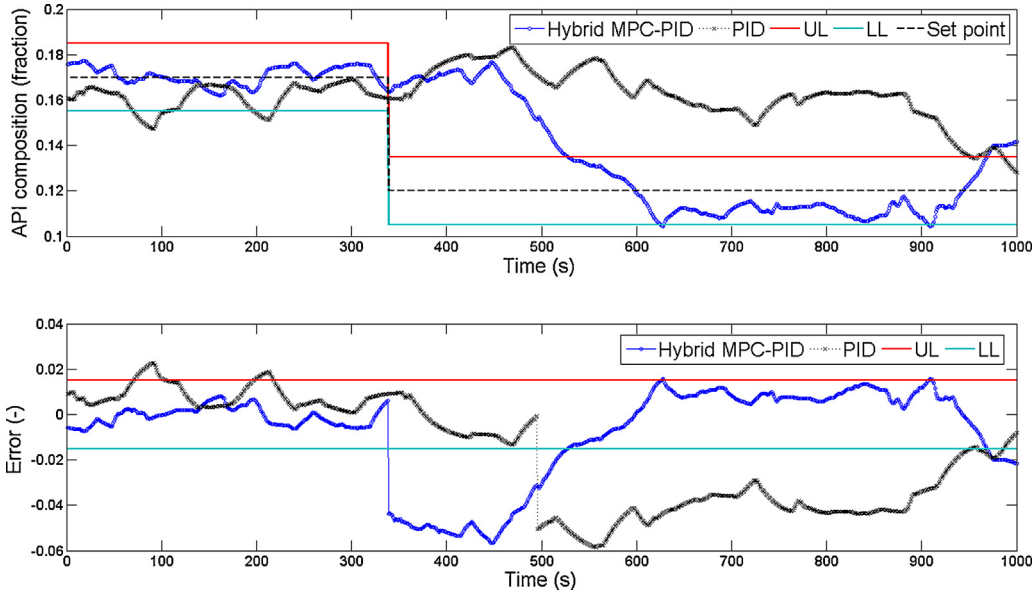

Fig. 14. Comparison of performance of hybrid MPC–PID control scheme with base level PID controller.

Table 4
Statistics of performance of implemented control system (experimental).

Criteria	PID	Hybrid MPC–PID
ITAE	14830.03 s	7757.77 s
RMSE	2.88%	2.12%
RSD	2.074%	0.984%

mean square error (RMSE) and relative standard deviation (RSD) has been calculated as given in Table 4. The ITAE value of hybrid MPC–PID control scheme was significantly less (around half) compared to PID control scheme. The root mean square error was also significantly less when the plant was running under hybrid MPC–PID control scheme compared to operational scenario where PID control scheme was used. The relative standard deviation which quantifies the blend uniformity is also significantly lower for hybrid MPC–PID based closed-loop operation than for PID based closed loop operation. It should be noted that the implemented control framework includes different options such as the option to run the plant in an open-loop or a closed-loop scenario. Furthermore, within the closed-loop scenario, options for a simpler PID, a dead time compensator (Smith predictor) and an advanced hybrid MPC–PID controller have been included so that the users can use any control system as per their convenience and availability of corresponding methods and tools. The feature to run the control strategy in simulation mode has also been added in the control platform that facilitates quick onsite control system design and performance evaluation (Singh et al., 2014b).

10. Conclusions

For the first time, a hybrid MPC–PID control system has been developed for a direct compaction continuous tablet manufacturing process. The PAT tools, control hardware and software integration and control system implementation have been demonstrated through a blending unit operation of continuous tablet manufacturing pilot plant. An NIR tool has been used for real time automatic hybrid MPC–PID based feedback blending process operation. An additional level of PCA based supervisory control system has been also integrated with hybrid MPC–PID based control architecture to identify the operational faults and to ensure the suitability of NIR data for control actions. The hybrid MPC–PID based control scheme shows better performance compared to a base level PID control scheme. A systematic flexible control framework for continuous tablet manufacturing process has been also developed with several novel features, including the option to run the plant in an open-loop or a closed-loop scenario. Furthermore, within the closed-loop scenario, options for a simpler PID, a dead time compensator (Smith predictor) and an advanced model predictive controller have been included. The feature to run the control strategy in simulation mode has been also added in the control platform that facilitates quick onsite control system design and performance evaluation. The current and future work includes the implementation of control loops into other unit operations of continuous tablet manufacturing process.

Acknowledgements

This work is supported by the National Science Foundation Engineering Research Center on Structured Organic Particulate Systems, through Grant NSF-ECC 0540855. The authors would also like to acknowledge Paul Brodbeck (CAI) for useful discussions.

Fig. A1. Continuous direct compaction tablet manufacturing pilot plant (adapted from Singh et al., 2012b).

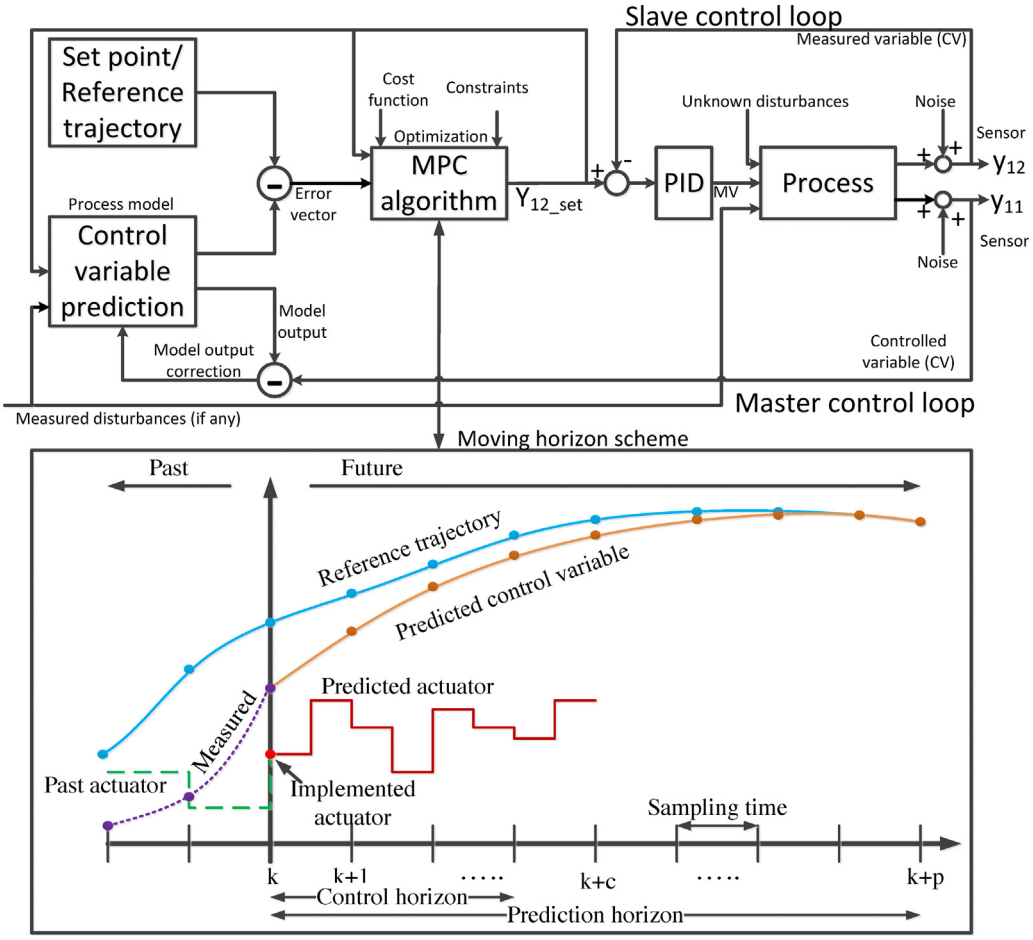

Fig. A2. Hybrid MPC–PID control structure. Bottom part of the figure shows the moving horizon scheme.

Appendix A.

A1. Pilot plant

The snapshot of the pilot plant is shown in Fig. A1 (whole plant is not shown).

A2. Hybrid MPC–PID control algorithm

Hybrid MPC–PID control strategy incorporates the advantages of basic PID control strategy as well as advanced model predictive controller. As shown in Fig. A2, in cascade hybrid mode, MPC is placed at supervisory level and provides the set point for slave PID controller. MPC is based on moving horizon scheme as shown in Fig. A2. Linear MPC uses a linear process model to predict the future value of control variable within the prediction horizon. As opposed to PID in MPC the error is a vector rather than a single point (Blevin et al., 2013). The set point can be either constant value or a time dependent trajectory. As shown in Fig. 2, the error vector is the deviation of model predicted control variable from the set point within the prediction horizon. This error vector is the input to the MPC control algorithm where the objective function has to be minimized taking into account past actuator (MPC output), input-output and process constraints and MPC tuning parameters. Optimization is performed within a prediction horizon and the MPC output is generated with a control horizon. The first data point of the MPC output provides the set point of slave PID controller and rest of the data points are disregarded. As shown in Fig. A2, the value of control variable (y_{11}) which is measured in real time through an inline/online sensor (e.g. NIR) and first data point of MPC output (y_{12_set}) are used to correct the model and plant mismatch. Therefore, the MPC is known to give a good performance even though the linear model is not very accurate and there exists a model-plant mismatch. However, an accurate linear model is always preferred to improve

Table A1
Direct compaction tablet manufacturing process model.

Process models	Useful references
Feeders	Boukouvala et al., 2012a
Mill	Barrasso et al., 2013a, 2013b
Blender	Sen et al., 2012, 2013; Sen and Ramachandran, 2012; Boukouvala et al., 2012b
Tablet press	Singh et al. 2010a; Kawakita and Ludde, 1971; Kuentz and Leuenberger, 2000
Dissolution	Kimber et al., 2011; Singh et al., 2012a
Integrated direct compaction line	Boukouvala et al., 2012; Singh et al., 2012a, 2013a

the MPC performance. If there are any known process disturbances that can be measured then these disturbances can be used as the input of MPC to take account of its effect on process in feed forward manner. There could be also some unknown process disturbances that will be rejected automatically through control action. The dynamic of slave control loop should be easier and fast so that a simple PID controller can track the set point generated by master MPC controller. The MPC sub-steps which include error vector generation, objective function (J) minimization, actuator trajectory generation, first data point implementation, control variable measurement, and model-plant mismatch correction is repeated for each time step therefore the MPC strategy is also called moving horizon scheme. Moving horizon scheme is also shown in Fig. A2. As shown in Fig. A2, the control variable is predicted with prediction horizon and the MPC output is generated within control horizon. The prediction horizon, control horizon is also shown in the figure.

The optimization function that needs to be minimized in MPC can be expressed as follows (Singh et al., 2013a):

$$J = \underbrace{\sum_{i=1}^{P}\sum_{j=1}^{n_y}\left\{w_j^y\left[y_j^{set}(k+i) - y_j(k+i)\right]\right\}^2}_{\text{(I)}} + \underbrace{\sum_{i=1}^{M}\sum_{j=1}^{n_u}\left\{w_j^{\Delta u}\Delta u_j(k+i-1)\right\}^2}_{\text{(II)}} + \underbrace{\sum_{i=1}^{M}\sum_{j=1}^{n_u}\left\{w_j^u\left[u_j(k+i-1) - \overline{u_j}\right]\right\}^2}_{\text{(III)}}$$

(I): the first term represents the weighted sum of squared deviations ($S_y(k)$). (II): the second term represents the weighted sum of controller adjustments ($S_{\Delta u}(k)$). (III): the third term represents the weighted sum of manipulated variable deviations ($S_u(k)$).

k: current sampling interval, $k+i$: future sampling interval (within the prediction horizon).

y_j: jth control variable, y_j^{set}: set point of jth variable, u_j: actuator for jth control variable.

P: number of control intervals in the prediction horizon. n_y: number of plant outputs.

$[y_j^{\text{set}}(k+i) - y_j(k+i)]$: predicted deviation for output j at interval $k+i$.

M: is the number of intervals in the control horizon. n_u: number of manipulated variables.

$\Delta u_j(k+i-1)$: predicted adjustment in manipulated variable j at the future (or current) sampling interval $k+i-1$.

$w^y{}_j$: weight for output j (the output weights let you dictate the accuracy with which each output must track its set point.

$w_i^{\Delta u}$: rate weight (it penalizes the incremental change rather than the cumulative value and increasing this weight forces the controller to make smaller, more cautious adjustments).

w_j^u: input weight (this weight helps to avoid large deviation from the nominal value of actuators).

$\overline{u_j}$: nominal value of actuator for input j.

A3. Process model of direct compaction tablet man manufacturing process

The process models of unit operations involved in direct compaction tablet manufacturing process are listed in Table A1.

References

Bardin, M., Knight, P.C., Seville, J.P.K., 2004. On control of particle size distribution in granulation using high-shear mixers. Powder Technol. 140, 169–175.

Barnes, R.J., Dhanoa, M.S., Lister, S.J., 1989. Standard normal variate transformation and de-trending of near-infrared diffuse reflectance spectra. Appl. Spectrosc. 43, 772–777.

Barrasso, D., Ramachandran, R., 2012. A comparison of model order reduction techniques for a four-dimensional population balance model describing multi-component wet granulation processes. Chem. Eng. Sci. 80, 380–392.

Barrasso, D., Walia, S., Ramachandran, R., 2013a. Multi-component population balance modeling of continuous granulation processes: a parametric study and comparison with experimental trends. Powder Technol. 241, 85–97.

Barrasso, D., Oka, S., Muliadi, A., Litster, J.D., Wassgren, C., Ramachandran, R., 2013b. Population balance model validation and prediction of CQAs for continuous milling processes: toward QbD in pharmaceutical drug product manufacturing. J. Pharm. Innov. 8, 147–162.

Blanco, M., Coello, J., Iturriaga, H., Maspoch, S., de la Pezuela, C., 1998. Nearinfrared spectroscopy in the pharmaceutical industry. Analyst 123, 135R–150R.

Blevins, T., Wojsznis, W.K., Nixon, M., 2013. Advanced control foundation. Tools, Techniques and Applications. International Society of Automation, NC, USA, pp. 1–978 ISBN: 978-1-937560-55-3.

Boukouvala, F., Chaudhury, A., Sen, M., Zhou, R., Mioduszewski, L., Ierapetritou, M., Ramachandran, R., 2013. Computer-aided flowsheet simulation of a pharmaceutical tablet manufacturing process incorporating wet granulation. J. Pharm. Innov. 8, 11–27.

Boukouvala, F., Niotis, V., Ramachandran, R., Muzzio, F., Ierapetritou, M., 2012a. An integrated approach for dynamic flowsheet modeling and sensitivity analysis of a continuous tablet manufacturing process: an integrated approach. Comput. Chem. Eng. 42, 30–47.

Boukouvala, F., Dubey, A., Vanarase, A., Ramachandran, R., Muzzio, F.J., Ierapetritou, M., 2012b. Computational approaches for studying the granular dynamics of continuous blending processes, 2 – population balance and data-based methods. Macromol. Mater. Eng. 297, 9–19.

Burggraeve, A., Tavares da Silva, A., van den Kerkhof, T., Hellings, M., Vervaet, C., Remon, J.P., vander Heyden, Y., Beer, T.D., 2012. Development of a fluid bed granulation process control strategy based on real-time process and product measurements. Talanta 100, 293–302.

Candolfi, A., de Maesschalck, R., Jouan-Rimbaud, D., Hailey, P.A., Massart, D.L., 1999. The influence of data pre-processing in the pattern recognition of excipients near-infrared spectra. J. Pharm. Biomed. Anal. 21, 115–132.

FDA, 2004. http://www.fda.gov/downloads/Drugs/ScienceResearch/ResearchAreas/ucm079290.pdf (accessed 03.03.14).

Gatzke, E.P., Doyle III, F.J., 2001. Model predictive control of a granulation system using soft output constraints and prioritized control objectives. Powder Technol. 121, 149–158.

Hsu, S., Reklaitis, G.V., Venkatasubramanian, V., 2010a. Modeling and control of roller compaction for pharmaceutical manufacturing. Part I: process dynamics and control framework. J. Pharm. Innov. 5, 14–23.

Hsu, S., Reklaitis, G.V., Venkatasubramanian, V., 2010b. Modeling and control of roller compaction for pharmaceutical manufacturing. Part II: control and system design. J. Pharm. Innov. 5, 24–36.

Jørgensen, A., 2000. Clustering excipient near infrared spectra using different chemometric methods. Pharmaceutical Technology Division, Department of Pharmacy, University of Helsinki. http://www.pharmtech.helsinki.fi/semi-naarit/vanhat/annajorgensen.pdf (accessed 14.01.00).

Kawakita, K., Ludde, K.H., 1971. Some considerations on powder compression equations. Powder Technol. 4, 61–68.

Kuentz, M., Leuenberger, H., 2000. A new model for the hardness of a compacted particle system, applied to tablets of pharmaceutical polymers. Powder Technol. 111, 143–145.

Kimber, J.A., Kazarian, S.G., Stepánek, F., 2011. Microstructure-based mathematical modelling and spectroscopic imaging of tablet dissolution. Comput. Chem. Eng. 35, 1328–1339.

Lavine, B.K., 1998. Chemometrics. Anal. Chem. 70, 209R–228R.

Long, C.E., Polisetty, P.K., Gatzke, E.P., 2007. Deterministic global optimization for nonlinear model predictive control of hybrid dynamic systems. Int. J. Robust Nonlin. Contr. 17, 1232–1250.

Muzzio, F., Singh, R., Chaudhury, A., Rogers, A., Ramachandran, R., Ierapetritou, M.G., 2013. Pharm. Tech. Mag. Eur. 37, 40–41 http://www.pharmtech.com/pharmtech/Manufacturing/Model-Predictive-Design-Control-and-Optimization/ArticleStandard/Article/detail/814906 (accessed 26.09.13).

Osborne, B.G., Fearn, T., Hindle, P.H., 1993. Practical NIR Spectroscopy with Applications in Food and Beverage Analysis, second ed. Longman Group, Burnt Mill, Harlow, Essex, England, UK pp. 20–33, 42–43, 106–113, 123–132.

PhRMA, 2012. Washington DC. http://phrma.org/sites/default/files/pdf/PhRMA%20Profile%202013.pdf (accessed 30.06.14).

Pottmann, M., Ogunnaike, B.A., Adetayo, A.A., Ennis, B.J., 2000. Model-based control of a granulation system. Powder Technol. 108, 192–201.

Portillo, P.M., Ierapetritou, M.G., Muzzio, F.J., 2008. Characterization of continuous convective powder mixing processes. Powder Technol. 368, 368–378.

Portillo, P.M., Ierapetritou, M.G., Muzzio, F.J., 2009. Effects of rotation rate, mixing angle, and cohesion in two continuous powder mixers — a statistical approach. Powder Technol. 194, 217–227.

Portillo, P.M., Vanarase, A., Ingram, A., Seville, J.K., Ierapetritou, M.G., Muzzio, F.J., 2010. Investigation of the effect of impeller rotation rate, powder flow rate, and cohesion on powder flow behavior in a continuous blender using PEPT. Chem. Eng. Sci. 65, 5658–5668.

Ramachandran, R., Chaudhury, A., 2012. Model-based design and control of continuous drum granulation processes. Chem. Eng. Res. Des. 90, 1063–1073.

Sanders, C.F.W., Hounslow, M.J., Doyle III, F.J., 2009. Identification of models for control of wet granulation. Powder Technol. 188, 255–263.

Seborg, D.E., Edgar, T.F., Mellichamp, D.A., 2004. Process Dynamics and Control, second ed. John Wiley & Sons, Inc..

Sen, M., Dubey, A., Singh, R., Ramachandran, R., 2013. Mathematical development and comparison of a hybrid PBM-DEM description of a continuous powder mixing process. J. Powder Technol. . http://dx.doi.org/10.1155/2013/843784.

Sen, M., Ramachandran, R., 2012. A multi-dimensional population balance model approach to continuous powder mixing processes. Adv. Powder Technol. 24, 51–59.

Sen, M., Singh, R., Vanarase, A., John, J., Ramachandran, R., 2012. Multi-dimensional population balance modeling and experimental validation of continuous powder mixing processes. Chem. Eng. Sci. 80, 349–360.

Singh, R., Gernaey, K.V., Gani, R., 2009. Model-based computer-aided framework for design of process monitoring and analysis systems. Comput. Chem. Eng. 33, 22–42.

Singh, R., Gernaey, K.V., Gani, R., 2010a. ICAS-PAT: a software for design, analysis and validation of PAT systems. Comput. Chem. Eng. 34, 1108–1136.

Singh, R., Gernaey, K.V., Gani, R., 2010b. An ontological knowledge based system for selection of process monitoring and analysis tools. Comput. Chem. Eng. 34, 1137–1154.

Singh, R., Ierapetritou, M.G., Ramachandran, R, 2012a. An engineering study on the enhanced control and operation of continuous manufacturing of pharmaceutical tablets via roller compaction. Int. J. Pharm. 438, 307–326.

Singh, R., Boukouvala, F., Jayjock, E., Ramachandran, R., Ierapetritou, M., Muzzio, F., 2012b. Flexible Multipurpose Continuous Processing of Pharmaceutical Tablet Manufacturing Process. GMP News, European Compliance Academic (ECE) http://www.gmp-compliance.org/ecanl_503_0_news_3268_7248_n.html (accessed 30.06.14).

Singh, R., Ierapetritou, M., Ramachandran, R., 2013a. System-wide hybrid model predictive control of a continuous pharmaceutical tablet manufacturing process via direct compaction. Eur. J. Pharm. Biopharm. 85, 1164–1182 Part B.

Singh, R., Godfrey, A., Gregertsen, B., Muller, F., Gernaey, K.V., Gani, R., Woodley, J.M., 2013b. Systematic substrate adoption methodology (SAM) for future flexible, generic pharmaceutical production processes. Comput. Chem. Eng. 58, 344–368.

Singh, R., Barrasso, D., Chaudhury, A., Sen, M., Ierapetritou, M., Ramachandran, R., 2014a. Closed-loop feedback control of a continuous pharmaceutical tablet manufacturing process via wet granulation. J. Pharm. Innov. 9, 16–37.

Singh, R., Sahay, A., Muzzio, F., Ierapetritou, M., Ramachandran, R., 2014b. Systematic framework for onsite design and implementation of the control system in continuous tablet manufacturing process. Comput. Chem. Eng. 66, 186–200.

Vanarase, A.U., Alcala, M., Rozo, J., Muzzio, F.J., Romanach, R.J., 2010. Real-time monitoring of drug concentration in a continuous powder mixing process using NIR spectroscopy. Chem. Eng. Sci. 65, 5728–5733.

Vanarase, A., Muzzio, F.J., 2011. Effect of operating conditions and design parameters in a continuous powder mixer. Powder Technol. 208, 26–36.

Vanarase, A., Gao, Y., Muzzio, F.J., Ierapetritou, M.G., 2011. Characterizing continuous powder mixing using residence time distribution. Chem. Eng. Sci. 66, 417–425.